

Regular Paper

Rapid BRDF Measurement Using an Ellipsoidal Mirror and a Projector

YASUHIRO MUKAIGAWA,^{†1} KOHEI SUMINO^{†1}
and YASUSHI YAGI^{†1}

Measuring a bidirectional reflectance distribution function (BRDF) requires long time because a target object must be illuminated from all incident angles and the reflected light must be measured from all reflected angles. In this paper, we introduce a rapid BRDF measuring system using an ellipsoidal mirror and a projector. Since the system changes incident angles without a mechanical drive, dense BRDF can be rapidly measured. Moreover, it is shown that the S/N ratio of the measured BRDF can be significantly increased by multiplexed illumination based on the Hadamard matrix.

1. Introduction

In recent years, the measurement of geometric information (3D shapes) has become easier by using commercial range-finders. However, the measurement of photometric information (reflectance properties) is still difficult. Reflection properties depend on the mesostructure of the surface, and they can be used for a variety of applications such as computer graphics and inspection of painted surfaces. However, there is no convenient way for measuring reflection properties.

The main reason for this is that the dense measurement of BRDFs requires huge amounts of time because a target object must be illuminated from every incident angle and the reflected lights must be measured from every reflected angle. Most conventional methods use mechanical drives to rotate a light source, and as a result, the measuring time becomes very long.

In this paper, we present a new method to measure BRDF rapidly. Our system substitutes an ellipsoidal mirror for a mechanical drive, and a projector for a light source. Since we completely exclude mechanical drive, high-speed measurement

can be realized. Our system can measure not only isotropic reflections but also anisotropic reflections defined by four angle parameters.

Moreover, we present an algorithm that improves the S/N ratio of measured BRDF. The combination of a projector and an ellipsoidal mirror can produce any illumination. Hence, the noise is significantly reduced by multiplexing illumination based on the Hadamard matrix, while the capturing time remains the same as for normal illumination.

2. Related Work

If the reflectance is uniform over the surface, the measurement becomes easier by merging the BRDFs at every point. For measuring isotropic BRDFs, Marschner, et al.¹⁾ used spherical samples, because the surface of a sphere has normals in all directions. To measure BRDFs of all curved near-convex objects, they used a 3D range scanner to acquire surface normal information²⁾. Matusik, et al.³⁾ measured BRDFs of spheres of more than 130 different materials. Anisotropic BRDFs can also be measured by capturing a plane⁴⁾ or a cylinder⁵⁾. Ngan, et al.⁶⁾ proposed a method to measure anisotropic BRDF in which a cylinder is wrapped with strips of the target material in different orientations.

The most straightforward way to measure BRDFs is to use a gonireflectometer, which allows a light source and a sensor to rotate around the target material. Li, et al.⁷⁾ have proposed a three-axis instrument. However, because the angle needs to be altered mechanically, the measurement of dense BRDFs takes a long time. To speed up the measurement, rotational mechanisms should be excluded. By placing many cameras and light sources around the target object, BRDFs can be measured for some of the angle combinations of the incident and reflective directions. Müller, et al.⁸⁾ have constructed a system including 151 cameras with a flash. However, dense measurement is physically difficult.

In the optics field, some systems that utilize catadioptric devices have been proposed. Davis and Rawling⁹⁾ have patented a system using an ellipsoidal mirror to collect the reflected light. Mattison, et al.¹⁰⁾ have developed a hand-held instrument based on the patent. The patent focuses only on gathering reflected light, and does not mention the control of the incident direction. Although Ward¹¹⁾

^{†1} Osaka University

Table 1 Comparison of major BRDF measuring devices.

Device	Camera	Light source	Density of BRDF
Li ⁷⁾	mechanical rotation	mechanical rotation	dense
Dana ¹²⁾	fixed	mechanical translation	dense
Müller ⁸⁾ , Han ¹⁴⁾	fixed	fixed	sparse
Ghosh ¹⁵⁾ , Our system	fixed	fixed	dense

used a hemi-ellipsoidal or hemispherical half-mirror and a fish-eye lens, it requires a rotational mechanism for the light source. Although Dana and Wang¹²⁾ used a paraboloidal mirror, a translational mechanism for the light source remains necessary.

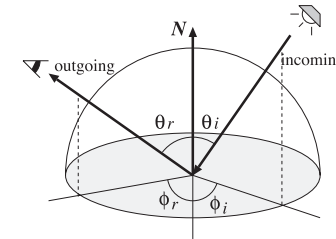
To avoid using mechanical drive, some systems include catadioptric devices. Kuthirummal and Nayar¹³⁾ used a cylindrical mirror and Han and Perlin¹⁴⁾ combined a projector and several plane mirrors similar to those used in a kaleidoscope. However, these systems can measure only sparse BRDFs because measurable incident and reflective angles are quite discrete. Recently, Ghosh, et al.¹⁵⁾ proposed a system that combines a paraboloidal mirror and a specially-designed dome mirror with a projector. The system can measure dense BRDFs without any mechanical drive. Because a target material cannot be observed from the surface normal direction owing to occlusion, a mechanism was provided to fill in the missing data using a zonal basis function.

We, on the other hand, propose a new system that combines an ellipsoidal mirror and a projector. Since our system completely excludes a mechanical device, high-speed measurement is realized. The system can measure dense BRDFs because both lighting direction and viewing direction are densely changed. The measurable angle for isotropic reflection is not limited by the horizontal setup. The comparison of major BRDF measuring devices is summarized in **Table 1**.

3. BRDF

3.1 Definition of BRDF

To represent reflection properties, the bidirectional reflectance distribution function (BRDF) is used. The BRDF represents the ratio of outgoing radiance in the viewing direction (θ_r, ϕ_r) to incident irradiance from a lighting direction (θ_i, ϕ_i) , as shown in **Fig. 1**. While the BRDF does in fact depend on wavelength,

**Fig. 1** Four angular parameters of BRDF.

it is sufficient to define the BRDF for each R, G, and B color channel for many applications such as computer graphics.

When a camera and a light source are fixed, the rotation of an object around the surface normal changes the appearance of some materials. Such reflection is called anisotropic reflection, and typical materials of this type are brushed metals and cloth fabrics such as velvet and satin. To perfectly describe anisotropic reflection, the BRDF should be defined by four angle parameters.

On the other hand, the appearance does not change according to the rotation around the surface normal for many materials. Such reflection is called isotropic reflection. If isotropic reflection can be assumed, the BRDF is described using three angle parameters, θ_i , θ_r , and ϕ ($\phi = \phi_i - \phi_r$). The isotropic BRDF is a subset of the anisotropic BRDF.

3.2 Problems of BRDF Measurement

When we measure dense BRDFs, we have to consider data size and measuring time. First, let us consider the data size for measuring anisotropic BRDFs. If the angles θ_r , ϕ_r , θ_i , and ϕ_i are rotated at one degree intervals, and the reflected light is recorded as R, G, and B colors for each angle, then the required data size becomes $360 \times 90 \times 360 \times 90 \times 3 = 3,149,280,000$ bytes. The size of 3 GB is not impractical for recent PCs. Moreover, BRDFs can be effectively compressed because they include much redundancy. Therefore, data size is not a serious problem.

On the other hand, the problem of measuring time remains serious. Since the number of combinations of lighting and sensing angles becomes extremely large, a long measuring time is required. If the sampling interval is one degree, the

total number of angular combinations becomes $360 \times 90 \times 360 \times 90 \simeq 10^9$. This means that it is impractical to measure dense BRDFs using a gonioreflectometer. In fact, Li, et al.⁷⁾ reported that the real measuring time becomes about 9-10 hours even if the number of angular configurations is 10^3 .

The estimation of the data size and measuring time mentioned above assumes the anisotropic reflection. If we can assume the isotropic reflection, the number of angle parameters can be reduced from four to three, then the measuring time and data size can be reduced. However, essential problem can not be solved.

Especially, the problem of measuring time warrants consideration, while the problem of data size is not serious. In this paper, we straightforwardly tackle the problem of measuring time by devising a catadioptric system.

4. BRDF Measuring System

4.1 Principle of Measurement

Conventional gonioreflectometers require huge amounts of time because mechanical drives are used for rotating the camera and light source around the target object. To realize high-speed measurement, such slow rotation mechanism should be excluded from the measuring system. Ward¹¹⁾ proposed the use of hemi-ellipsoidal mirror to collect reflected light. Hence, we also utilize an ellipsoidal mirror instead of the rotation mechanism.

An ellipsoid has two focal points. All rays from one focal point reflect off the ellipsoidal mirror and reach the other focal point as shown in **Fig. 2**. This property is used for measuring BRDFs. The target object is placed at the focal point, and a camera is placed at the other focal point. Since rays reflected in all directions from the target object converge at a single point, all the rays can be captured using a camera at once. This means that all reflected rays can be recorded as an image without using a rotation mechanism.

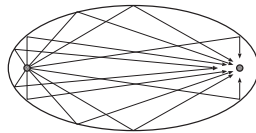


Fig. 2 Two focal points of ellipsoid.

The most significant characteristic of the system is that the ellipsoidal mirror is combined with a projector. By placing the projector at the focal point of the ellipsoidal mirror, the projector serves as a substitute for the light source. That is, the projection of a pattern in which only one pixel is white corresponds to the illumination by a point light source. Moreover, changing the location of the white pixel corresponds to rotating the incident angle. Since the change of the projection pattern is faster than mechanical rotation, rapid and dense measurement can be achieved.

4.2 Design of the Measuring Systems

Based on the principle described in the previous section, we designed two setups that have differently shaped ellipsoidal mirrors. One is a vertical setup in which a target material is placed vertically to the long axis as shown in **Fig. 3** (a). The shape of the mirror is an ellipsoid that is cut perpendicularly to the long axis as shown in **Fig. 4** (a). The other is a horizontal setup in which a target material is placed horizontally to the long axis as shown in **Fig. 3** (b). The shape of the mirror is an ellipsoid that is cut parallel and perpendicularly to the long axis as shown in **Fig. 4** (b).

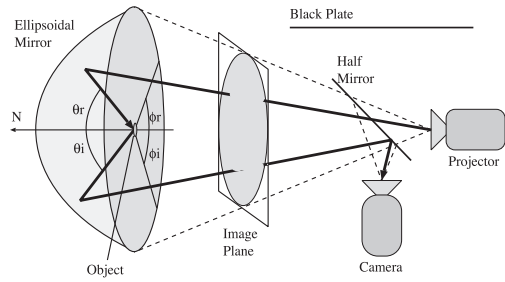
The major optical devices are a projector, a digital camera, an ellipsoidal mirror, and a beam splitter. The illumination from the projector is reflected on the beam splitter and the ellipsoidal mirror, and finally illuminates a single point on the target object. The reflected light on the target object is again reflected by the ellipsoidal mirror, and is recorded as an image.

The vertical setup has merit in that the density of the BRDF is uniform along ϕ because the long axis of the ellipsoid and the optical axes of the camera and projector are the same. Moreover, this kind of mirror is available commercially because it is often used as part of a usual illumination device. However, target materials must be cut into small facets to be placed at the focal point.

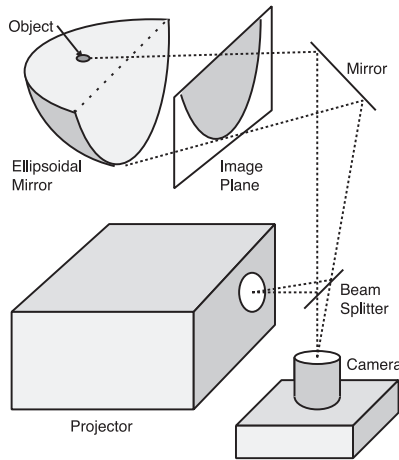
On the other hand, the horizontal setup has merit in that the target materials do not have to be cut. Hence, the BRDF of cultural heritages can be measured. However, the mirror must be specially made by the cutting operation.

4.3 Measurable Angles

The lighting and viewing directions are specified as angles, while they are expressed as 2-D locations in the projection pattern or the captured image. The



(a) Vertical setup



(b) Horizontal setup

Fig. 3 The design of the BRDF measuring system.

conversion between the angle and the image location is easy if geometric calibration is done for the camera and the projector. **Figures 5** (a) and (b) illustrate the relationship between the angle and the image location for the vertical and horizontal setup, respectively.

In the case of the vertical setup, a small facet of the target material occludes some rays. From the surface normal direction, the target material cannot be illuminated and the reflected lights cannot be observed. Hence, the BRDF near the surface normal cannot be measured. These immeasurable angles correspond

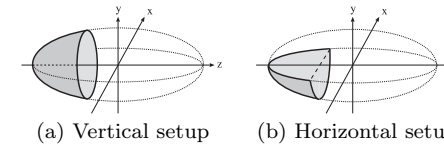


Fig. 4 The shape of the ellipsoidal mirror.

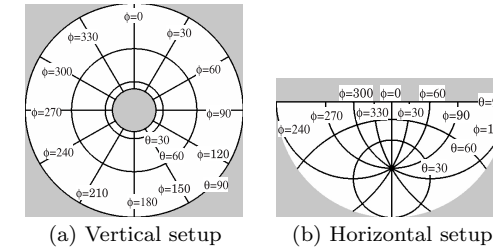


Fig. 5 Relationship between the angles (θ , ϕ) and the image location.

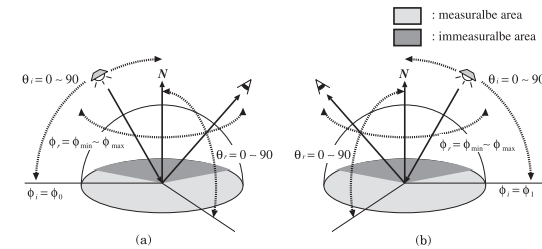


Fig. 6 Measurement of isotropic BRDF by the horizontal setup. (a) $\phi_i = \phi_0$. (b) $\phi_i = \phi_1$.

to the center area of Fig. 5 (a).

On the other hand, the target material is placed without cutting so that a certain point on the surface corresponds to the focal point of the ellipsoidal mirror in the case of the horizontal setup. That is, the target material does not disturb the illumination and observation, even if the size of target material is large. Hence, the isotropic BRDF can be fully measured without any missing data. The isotropic BRDF depends only on the relative angle ($\phi_i - \phi_r$). That is, the azimuth angle ϕ_i can be fixed to ϕ_0 , and the lighting direction is limited to a quarter of the circular arc of $0 \leq \theta_i \leq 90$ as shown in **Fig. 6** (a). However,

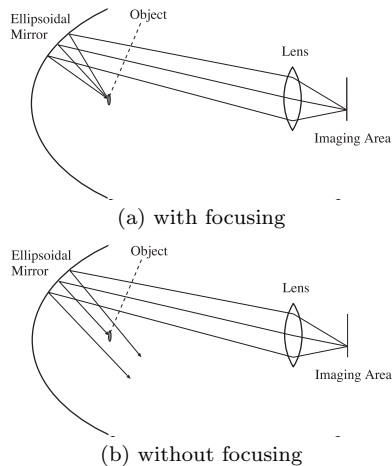


Fig. 7 Light path from projector.

the BRDFs of only $0 \leq \theta_r \leq 90$ and $\phi_{min} \leq \phi_r \leq \phi_{max}$ can be measured according to the shape of the ellipsoidal mirror. Hence, we set ϕ_i to two angles of ϕ_0 and ϕ_1 and merge the two BRDFs as shown in Fig. 6 (b). If the condition of $\phi_{max} - \phi_{min} \geq 180$ is satisfied, we can set $\phi_0 = 0$ and $\phi_1 = 180$. Consequently, full isotropic BRDFs without any immeasurable angles can be obtained by varying the lighting direction along a half of the circular arc of $0 \leq \theta_i \leq 180$.

4.4 Focusing and Aperture

We now consider the optical settings of the projector and camera. Ideally, the aperture should be a pinhole because each ray corresponds to an incident or outgoing angle. For the camera, such settings can be easily realized. However, it is difficult to change the aperture of the projector because we cannot replace the lenses of commercially-available projectors. **Figure 7** (a) illustrates the light path from the projector if the rays are focused on the target object. In this case, one pixel in the projecting pattern is observed as a light source having a large solid angle. The solid angle is determined by the size of the lens. To avoid this undesired effect, the rays from the projector are focused at infinity, as shown in Fig. 7 (b). Through the defocusing of the projection, the light source is observed as a point from the position of the target object.

5. Multiplexed Illumination

In this section, we clarify the problem of low S/N ratio inherent in the proposed system, and we show that the S/N ratio can be improved by multiplexed illumination based on the Hadamard matrix.

5.1 S/N Ratio

In general, specular reflection is much brighter than diffuse reflection. In our measurement system, both specular and diffuse reflections are recorded in the same image simultaneously. If the dynamic range of the camera is limited, a long shutter speed causes saturation of the specular reflection. Conversely, if a short shutter speed is used to avoid saturation due to limited dynamic range, diffuse reflection becomes extremely dark. If the noise level is high compared with the diffuse reflection, the S/N ratio tends to be very low. Hence, a radical solution is required.

5.2 Multiplexed Illumination

Optical multiplexing techniques from the 1970s have been investigated in the spectrometry field¹⁶⁾. If the spectrum of a light beam is measured separately for each wavelength, each spectral signal becomes noisy. Using the optical multiplexing technique, multiple spectral components are simultaneously measured to improve the quality. In the computer vision field, Schechner, et al.¹⁷⁾ applied the multiplexing technique to capture images under varying illumination. In this method, instead of illuminating each light source independently, the multiplexed light sources are simultaneously illuminated. From the captured images, an image that is illuminated by a single light source is calculated. Wenger, et al.¹⁸⁾ evaluated the effects of noise reduction using multiplexed illumination.

We briefly describe the principle of multiplexed illumination. Let us assume that there are n light sources, and that \mathbf{s} denotes the intensities of a point in the images when each light source turns on. The captured images are multiplexed by the weighting matrix \mathbf{W} . The intensities \mathbf{m} of the point by the multiplexed illumination are expressed by

$$\mathbf{m} = \mathbf{W}\mathbf{s}. \quad (1)$$

The intensities of the point under the single illumination can be estimated by

$$\mathbf{s} = \mathbf{W}^{-1}\mathbf{m}. \quad (2)$$

In our BRDF measuring system, a projector is used instead of an array of light sources. Hence the weighting matrix \mathbf{W} can be arbitrarily controlled. It is known that if the component of the matrix \mathbf{W} is -1 or 1 , the Hadamard matrix is the best multiplexing weight¹⁶⁾. In this case, the S/N ratio is increased by a factor of \sqrt{n} . The $n \times n$ Hadamard matrix satisfies

$$\mathbf{H}_n^T \mathbf{H}_n = n \mathbf{I}_n, \quad (3)$$

where \mathbf{I}_n denotes an $n \times n$ identity matrix.

In fact, as negative illumination cannot be given by a projector, the Hadamard matrix cannot be used directly. It is also known that if the component of the matrix \mathbf{W} is 0 or 1 , the S -matrix is the best multiplexing weight¹⁶⁾. In this case, the S/N ratio is increased by a factor of $\sqrt{n}/2$. The S -matrix can be easily generated from the Hadamard matrix.

Hence, the projection pattern is multiplexed using the S -Matrix. Since the illumination can be controlled for each pixel using a projector, n becomes a large number and dramatic improvement can be achieved.

6. Experimental Results

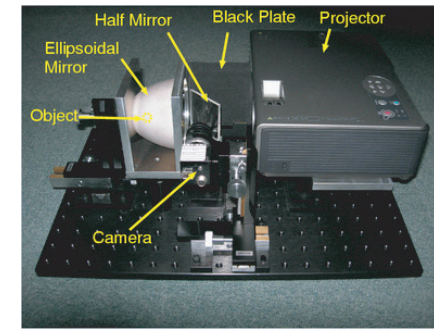
6.1 BRDF Measuring Systems

We constructed two BRDF measuring systems named RCGs (Rapid Catadioptric Gonioreflectometers) as shown in **Fig. 9**. The RCG-1 includes a PointGrey Flea camera, an EPSON EMP-760 projector, and a Melles Griot ellipsoidal mirror as shown in **Fig. 8** (a). Since this ellipsoidal mirror has a hole at the edge of the long axis, the BRDFs within $0 \leq \theta_i, \theta_r \leq 27$ cannot be measured. A small facet of the target object is placed through the hole using a piano wire.

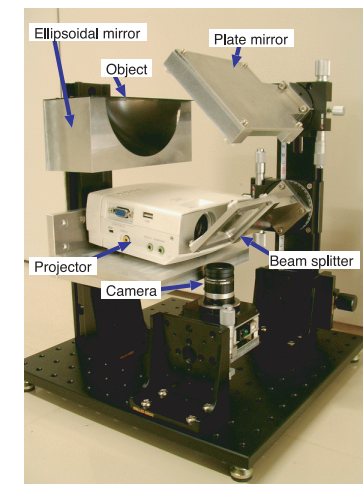


Fig. 8 The ellipsoidal mirrors.

The RCG-2 includes a Lucam Lw-160C camera and a TOSHIBA TDP-FF1A projector. The ellipsoidal mirror for the RCG-2 is designed so that BRDFs can be measured for all angles of θ within $0 \leq \phi \leq 240$ as shown in Fig. 8 (b). Since the projector is battery-driven, BRDFs can be measured outdoors by combining with a laptop PC.



(a) RCG-1 (vertical setup)



(b) RCG-2 (horizontal setup)

Fig. 9 The BRDF measuring systems.

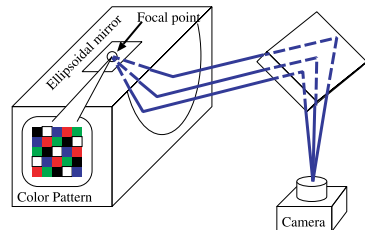


Fig. 10 The alignment of the camera.

6.2 Optical Alignment

In general, radiometric calibration is important for projector-camera systems. However, the estimation of the response function is not necessary in our system because the projecting pattern includes only white and black pixels, and no gray levels are projected. We do not have to consider the nonlinearity of the projected luminance to the input signal. We assume that the illumination field is uniform over the incident angles. The calibration of the illumination field is our future work because it may affect the results.

On the other hand, geometric calibration is unnecessary because the placement of optical devices such as the camera, the projector, and mirrors is based on the system design. However, the geometric alignment should be strictly checked. That is, we have to confirm whether all optical devices are accurately placed based on the design. We introduce our empirical processes to align the optical devices. Since the same way was used for both RCG-1 and RCG-2, we describe the process used for RCG-2 due to space limitations.

For checking the camera alignment, we used a small patch on which several colors are printed as shown in **Fig. 10**. If the camera alignment is accurate, only one color is observed over the image area because the camera observes a single point. The position of the camera is aligned so that one color is observed over the image area.

For checking the projector alignment, we projected a particular pattern as shown in **Fig. 11**. The position of the projector is aligned so that the contour pattern of the ellipsoid corresponds to cross-section of the ellipsoid.

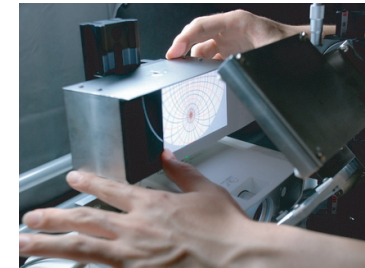


Fig. 11 The alignment of the projector.

6.3 Isotropic BRDF

First of all, we measured isotropic BRDFs to confirm the availability of the proposed device. The first target objects are penny coins as shown in **Figs. 12** (a) and (b). One is an old penny and the other is a new glossy one. Since these coins have isotropic reflection, the RCG-2 was used to measure full BRDF without missing angle. In this case, the lighting direction is varied by 1-DOF rotation because of the isotropic reflection. That is, the azimuth angle ϕ_i is fixed, and the elevation angle is varied $0 \leq \theta_i \leq 180$. To reduce image noise, ten images are captured for each illumination angle and the averaged values are stored. It takes about 6 minutes to measure BRDFs at one degree intervals.

Using measured BRDFs, CGs of a dragon shape²⁰⁾ are rendered. We extended the POV-Ray²¹⁾, which is ray tracing software, so that the measured raw BRDF data are directly used for rendering. Figures 12 (c) and (d) show the synthesized images using BRDFs of the old and new penny coins, respectively. We can see that reflection properties of each coin are appropriately reproduced.

Next, we compared rendered images with real ones taken under the same conditions. For this comparison we used two different kinds of papers, red metallic paper and blue fancy paper as shown in **Fig. 13** (a). The isotropic BRDFs were measured using the RCG-2 in the same way as for the penny coins. The papers are wrapped around a cylinder and real images are taken in a dark room using an LED point light source. The corresponding synthetic images are rendered under the same conditions as for the real images. Figures 13 (b) and (c) compare real images and synthesized images. The left images are real images and the

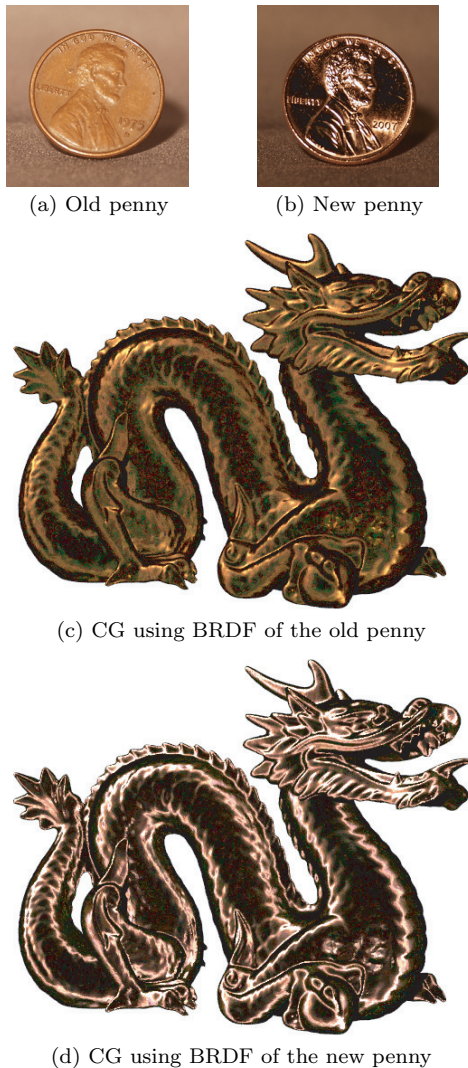
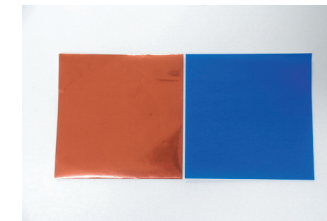
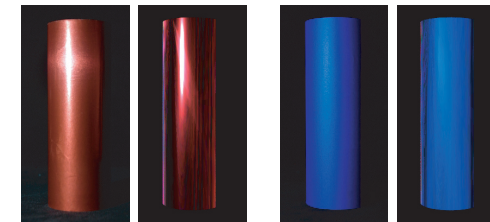


Fig. 12 Rendering results of penny coins.



(a) Target papers



(b) Red paper

(c) Blue paper

Fig. 13 Visual comparison of two different papers.

right images are synthesized images, respectively. We can see that the diffuse reflections are not smooth compared with the real images. This means that the measured reflectance is unstable. The possible reasons are image noise, inaccurate alignment of the optical devices, and scratch of the ellipsoidal mirror. On the other hand, the distribution of specular reflections is well reproduced.

6.4 Anisotropic BRDF

Next, anisotropic BRDFs which are defined by four angle parameters were measured. For this purpose, the RCG-1 is used because it can measure BRDFs with uniform angular density along ϕ . The target objects are velvet and satin, both of which have anisotropic reflections, as shown in Fig. 14. The sampling interval was set to one degree.

Figure 15 shows examples of captured images of velvet and satin when the pattern corresponding to the lighting directions $\theta_i = 30$ and $\phi_i = 250$ was projected. It is noted that some BRDFs could not be measured because the ellipsoidal mirror has a hole. Totally $360 \times 90 = 32,400$ images were captured for each material. The measuring time was about 50 minutes. A major part of the measuring time

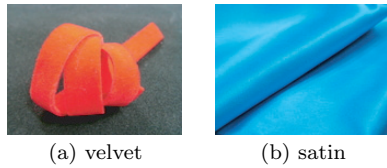


Fig. 14 Cloth with anisotropic reflection.

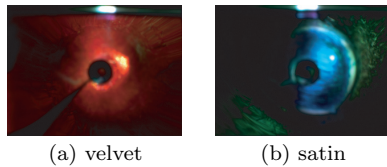


Fig. 15 Examples of captured images.

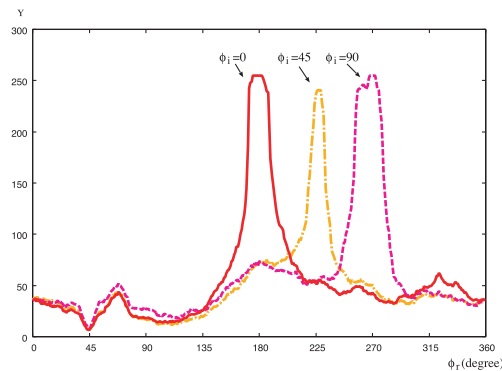


Fig. 16 Reflectance of velvet.

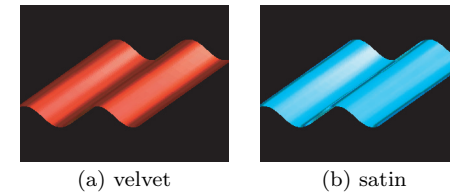


Fig. 17 Rendering results of velvet and satin.

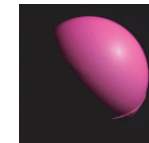


Fig. 18 Polyurethane sphere.

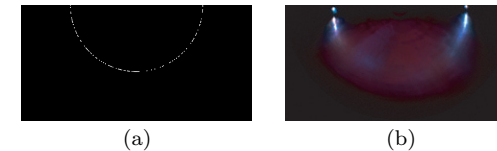


Fig. 19 An example of the multiplexed illumination. (a) projected pattern multiplexed by a 191×191 S-Matrix, and (b) the captured image.

was occupied by the process of preparing the projection pattern and recording the captured image.

Figure 16 shows the change of reflection intensities of the velvet material when θ_r is fixed to 30 degrees and ϕ_r rotates from 0 to 360 degrees. In the graph, the three lines show the respective reflection intensities for the lighting direction (θ_i, ϕ_i) : $(30, 0)$, $(30, 45)$, and $(30, 90)$. We can see that the three lines have different shapes at their peaks which represent the characteristics of the specular

reflection. Since the velvet material has anisotropic reflection properties, the reflectance varies even if the relative angle $(\phi_r - \phi_i)$ is the same.

Figure 17 are generated images of a corrugated plane that have the measured BRDFs of velvet and satin. The rendering process for this corrugated shape fortunately does not require the missing data. It can be seen that the characteristics of anisotropic reflection are reproduced.

6.5 Multiplexed Illumination

To evaluate the effectiveness of the multiplexed illumination, the isotropic BRDF of a polyurethane sphere was measured as shown in Figure 18. Figure 19 (a) shows an example of multiplexed illumination by a 191×191 S-matrix, and (b) shows the captured image after subtracting an image of projecting a black pattern.

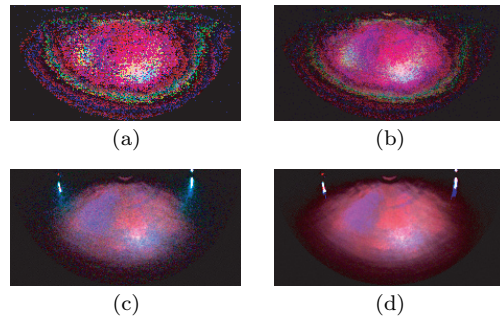


Fig. 20 The reflected light of the lighting direction ($\theta_l = 10, \phi_l = 270$). (a) single illumination without averaging, (b) single illumination with averaging, (c) multiplexed illumination without averaging, (d) multiplexed illumination with averaging.

The captured images of the lighting direction $\theta_i = 10, \phi_i = 270$ were compared under several conditions. **Figures 20** (a) and (b) show the distribution of the reflected light without multiplexing. (a) is a single captured image, while (b) is the average of ten captured images. These images are very dark because the object is lit by weak illumination. Hence the images are shown brightly for better visualization. The captured images are very noisy even with the averaging process. Figures 20 (c) and (d) show the results with multiplexing. A sequence of multiplexed illumination patterns were projected, and the distribution of the reflected light corresponding to the same lighting direction is estimated. As before, (c) is the result without averaging, while (d) is the result with averaging ten images. Obviously, the noise is dramatically decreased in the multiplexed illumination.

To find the spatial distribution of the reflected light, the changes in intensity of $y = 60, 30 \leq x \leq 200$ are plotted as shown in **Fig. 21**. (a) shows the intensities without averaging, while (b) shows those with averaging ten images. In the graphs, blue and red lines represent the distribution with and without multiplexing, respectively. It is interesting that the result of multiplexing without averaging is more accurate than the result of the single illumination with averaging. While the time taken for capturing images is ten times greater for the averaging process, the multiplexed illumination can improve accuracy without increasing the capturing time.

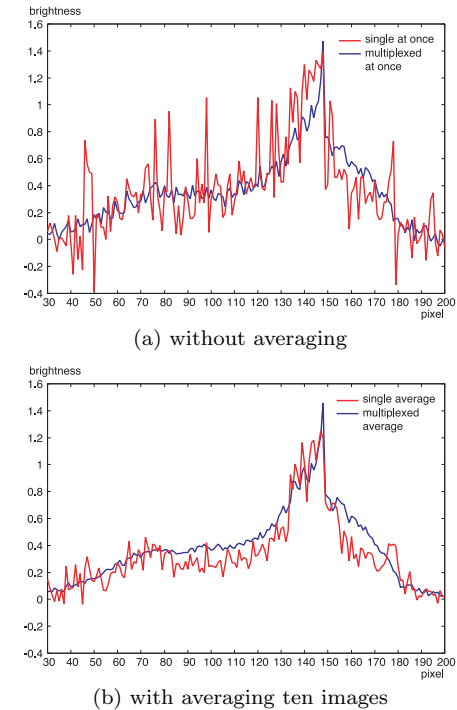


Fig. 21 The distribution of the intensities.

Figure 22 shows rendered images of a sphere and a corrugated surface using the BRDF measured by multiplexed illumination with averaging. Compared with the real sphere, the specular reflection is strong and the distribution is slightly wide. One of the reasons for this is that the light reflecting on the ellipsoidal mirror does not converge perfectly on the target material, because the alignment of the optical devices is not perfect. Because the target object is a sphere, the normal direction varies if the measuring point is different. As a result, wide specular reflections may be generated incorrectly. Moreover, the rendered images are still noisy. One of the possible reasons for this is that the optical path depends on the wavelength in our system. That is, red and blue rays emitted from the projector do not illuminate the same point. In fact, incorrect colors are observed

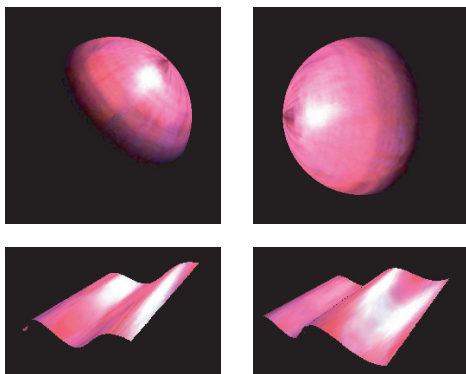


Fig. 22 Rendering results of the pink polyurethane sphere.

in Fig. 20, while the color of the target material is pink. The alignment of the optical devices will be the most important aspect of future work.

7. Conclusion

In this paper, we proposed a new high-speed BRDF measurement method that combines an ellipsoidal mirror with a projector, and solved the low S/N ratio problem by applying multiplexed illumination to pattern projection. Two BRDF measuring systems were developed, which include differently shaped ellipsoidal mirrors. The proposed systems can measure complex reflection properties including anisotropic reflection. Moreover, the measuring time of BRDFs can be significantly shortened by the exclusion of a mechanical device.

This paper focuses only on the BRDF measuring speed of the developed systems. The accuracy of the measured BRDFs needs to be evaluated. For the evaluation, we are attempting to compare the measured BRDFs and the ground truth using reflectance standards for which reflection properties are known.

While the low S/N ratio problem is reduced using multiplexed illumination, the narrow dynamic range problem is still unsolved. That is, both extremely bright specular reflections and dark diffuse reflections cannot be measured with satisfactory accuracy. The dynamic range may be widened by incorporating the use of several images captured with varying shutter speeds¹⁹⁾, while the capturing

time increases. The HDR measurement is one of our future works.

This work is supported by the Special Coordination Funds for Promoting Science and Technology of Ministry of Education, Culture, Sports, Science and Technology.

References

- 1) Marschner, S.R., Westin, S.H., Lafortune, E.P.F. and Torrance, K.E.: Image-Based Bidirectional Reflectance Distribution Function Measurement, *Applied Optics*, Vol.39, No.16, pp.2592–2600 (2000).
- 2) Marschner, S.R., Westin, S.H., Lafortune, E.P.F., Torrance, K.E. and Greenberg, D.P.: Image-Based BRDF Measurement Including Human Skin, *Proc. 10th Eurographics Workshop on Rendering*, pp.139–152 (1999).
- 3) Matusik, W., Pfister, H., Brand, M. and McMillan, L.: A Data-Driven Reflectance Model, *Proc. SIGGRAPH2003*, pp.759–769 (2003).
- 4) Karner, K.F., Mayer, H. and Gervautz, M.: An image based measurement system for anisotropic reflection, *Computer Graphics Forum (Eurographics'96 Proceedings)*, Vol.15, Issue 3, pp.119–128 (1996).
- 5) Lu, R., Koenderink, J.J. and Kappers, A.M.L.: Optical Properties (Bidirectional Reflection Distribution Functions) of Velvet, *Applied Optics*, Vol.37, No.25, pp.5974–5984 (1998).
- 6) Ngan, A., Durand, F. and Matusik, W.: Experimental Analysis of BRDF Models, *Proc. Eurographics Symposium on Rendering 2005*, pp.117–126 (2005).
- 7) Li, H., Foo, S.C., Torrance, K.E. and Westin, S.H.: Automated three-axis gonioreflectometer for computer graphics applications, *Proc. SPIE*, Vol.5878, pp.221–231 (2005).
- 8) Müller, G., Bendels, G.H. and Klein, R.: Rapid Synchronous Acquisition of Geometry and Appearance of Cultural Heritage Artefacts, *VAST2005*, pp.13–20 (2005).
- 9) Davis, K.J. and Rawlings, D.C.: Directional reflectometer for measuring optical bidirectional reflectance, United States Patent 5637873 (June 1997).
- 10) Mattison, P.R., Dombrowski, M.S., Lorenz, J.M., Davis, K.J., Mann, H.C., Johnson, P. and Foos, B.: Handheld directional reflectometer: An angular imaging device to measure BRDF and HDR in real time, *Proc. SPIE*, Vol.3426, pp.240–251 (1998).
- 11) Ward, G.J.: Measuring and Modeling anisotropic reflection, *Proc. SIGGRAPH'92*, pp.255–272 (1992).
- 12) Dana, K.J. and Wang, J.: Device for convenient measurement of spatially varying bidirectional reflectance, *J. Opt. Soc. Am. A*, Vol.21, Issue 1, pp.1–12 (2004).
- 13) Kuthirummal, S. and Nayar, S.K.: Multiview Radial Catadioptric Imaging for Scene Capture, *Proc. SIGGRAPH2006*, pp.916–923 (2006).
- 14) Han, J.Y. and Perlin, K.: Measuring Bidirectional Texture Reflectance with a

- Kaleidoscope, *ACM Transactions on Graphics*, Vol.22, No.3, pp.741–748 (2003).
- 15) Ghosh, A., Achutha, S., Heidrich, W. and O’Toole, M.: BRDF Acquisition with Basis Illumination, *Proc. ICCV2007* (2007).
 - 16) Harwit, M. and Sloane, N.J.A.: HADAMARD TRANSFORM OPTICS, ACADEMIC PRESS (1973).
 - 17) Schechner, Y.Y., Nayar, S.K. and Belhumeur, P.N.: A Theory of Multiplexed Illumination, *Proc. ICCV2003*, pp.808–815 (2003).
 - 18) Wenger, A., Gardner, A., Tchou, C., Unger, J., Hawkins, T. and Debevec, P.: Performance Relighting and Reflectance Transformation with Time-Multiplexed Illumination, *Proc. SIGGRAPH2005*, pp.756–764 (2005).
 - 19) Debevec, P. and Malik, J.: Recovering High Dynamic Range Radiance Maps from Photographs, *Proc. SIGGRAPH1997*, pp.369–378 (1997).
 - 20) The Stanford 3D Scanning Repository, <http://graphics.stanford.edu/data/3Dscanrep/>.
 - 21) POV-Ray, <http://www.povray.org/>.

(Received February 28, 2008)

(Accepted September 24, 2008)

(Released January 30, 2009)

(Communicated by *Yasuyuki Matsushita*)



Yasuhiro Mukaigawa received his M.E. and Ph.D. degrees from University of Tsukuba in 1994 and 1997, respectively. He became a research associate at Okayama University in 1997, an assistant professor at University of Tsukuba in 2003, and an associate professor at Osaka University in 2004. His current research interests include photometric analysis and computational photography. He was awarded the MIRU Nagao Award in 2008. He is a member of IEICE, VRSJ, and IEEE.



Kohei Sumino received his M.E. degree from Osaka University in 2007. He is currently working for Recruit Agent Co., Ltd.



Yasushi Yagi is the Professor of Intelligent Media and Computer Science, and the Assistant Director of the Institute of Scientific and Industrial Research, Osaka university, Ibaraki, Japan. He received his Ph.D. degree from Osaka University in 1991. In 1985, he joined the Product Development Laboratory, Mitsubishi Electric Corporation, where he worked on robotics and inspections. He became a research associate in 1990, a lecturer in 1993, an associate professor in 1996, and a professor in 2003 at Osaka University. The international conferences for which he served as chair include: FG1998 (Financial chair), OMINVIS2003 (Organizing chair), ROBIO2006 (Program co-chair), ACCV2007 (Program chair), PSVIT2009 (Financial chair) and ACCV2009 (General chair). He is the editor of IEEE ICRA Conference Editorial Board (2007, 2008), the editor in chief of IPSJ Transactions on Computer Vision & Image Media, and the associate editor in chief of IPSJ Transactions on Computer Vision & Applications. He was awarded ACM VRST2003 Honorable Mention Award, IEEE ROBIO2006 Finalist of T.J. Tan Best Paper in Robotics, IEEE ICRA2008 Finalist for Best Vision Paper, and MIRU2008 Nagao Award. His research interests are computer vision, medical engineering and robotics. He is a member of IEICE, RSJ, and IEEE.